

S1. The Federal Equivalency Method (FEM) in situ sites.

Fig. S1b shows the diel variation of the nine types of instruments used at FEM in-situ sites, which provide hourly measurements of $\text{PM}_{2.5}$ across the US. The number and location of instrument types are in Fig. 1. The majority (90.2%) of these instruments belongs to the first four kinds, which are shown in Fig. S1a. They exhibit generally consistent average diel profile of measured $\text{PM}_{2.5}$ masses, which we target as the typical variation to investigate. The other five types, shown as colored or dashed curves in Fig. S1b, are more deviated from the typical profiles. Specifically, the Teledyne Model 602 measures $\text{PM}_{2.5}$ concentrations variability which largely deviates from the typical pattern in Fig. S1a. The GRIMM Model 180 measures a pronounced morning peak. The Met One BAM-1022 shows a morning minimum of $\text{PM}_{2.5}$. The TEOM 1400 measures notably lower concentrations from midnight to early morning. Considering that these five types of instruments with deviated $\text{PM}_{2.5}$ diel patterns only account for less than 10% in all types, we exclude them from our analysis. Our analysis focuses on investigating the typical diel cycles in Fig. S1a.

S2. Spatial distribution of $\text{PM}_{2.5}$ in GEOS-Chem simulations and in situ measurements

Fig. S2a maps the annual $\text{PM}_{2.5}$ concentrations over the US simulated by the GC_Base simulation with the FEM/FRM in-situ measurements overlaid. The observed $\text{PM}_{2.5}$ concentrations are elevated over large parts of the Eastern US and the west coast. Other regions, primarily the mountainous Midwest, have relatively lower $\text{PM}_{2.5}$ levels with annual average concentrations below $10 \mu\text{g}/\text{m}^3$. Nevertheless, local hotspots can still be identified for major cities (Denver, the Salt Lake City, Phenix) and national forests vulnerable to open fires (Nez Perce-Clearwater near the state boundary of Idaho/Montana, Okanogan-Wenatchee in north WA). The GC_Base simulation broadly captures the observed spatial variation of annual mean $\text{PM}_{2.5}$ over the US in 2016 with the Root Mean Square Deviations (RMSD) against the FRM/FEM in-situ measurements of $4.88/4.31 \mu\text{g}/\text{m}^3$. The statistics for the FEM and FRM sites are consistent, providing a measure of confidence in the data quality of the hourly FEM measurements. The simulated concentrations are systematically biased high against observations by 44%. The contributors to this bias are peripherally explored but are not the main focus of this work. Fig. S2b maps the annual concentrations by the GC_2m simulation, in which temporal resolution of emissions is increased from monthly to hourly, dry deposition scheme is updated and the vertical representativeness differences between model and observations are resolved. The RMSD of the GC_2m $\text{PM}_{2.5}$ against the FEM/FRM measurements drop from $4.88/4.31$ to $4.08/3.66 \mu\text{g}/\text{m}^3$. The overestimates of $\text{PM}_{2.5}$ in Eastern US and the west coast are notably reduced. These results indicate that our model updates not only improve on the simulation of diel $\text{PM}_{2.5}$ mass variations, but also on annual mean concentrations.

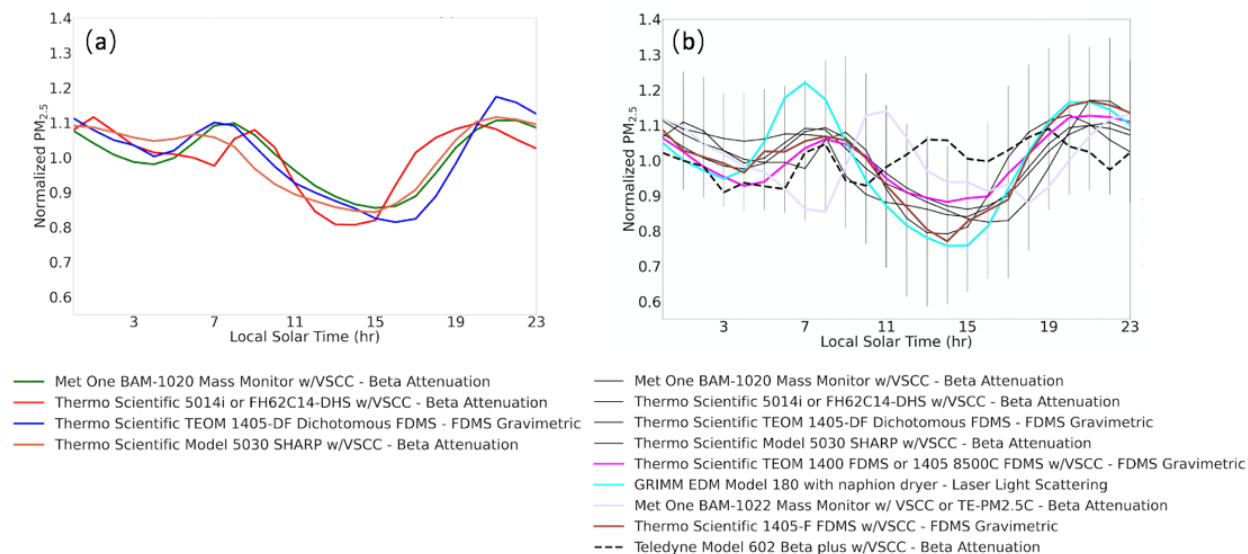


Figure S1. Averaged diel $PM_{2.5}$ variations of different FEM in-situ instruments over the US in 2016. (a) The major four types of instruments with typical diel $PM_{2.5}$ cycles. (b) All types of instruments.

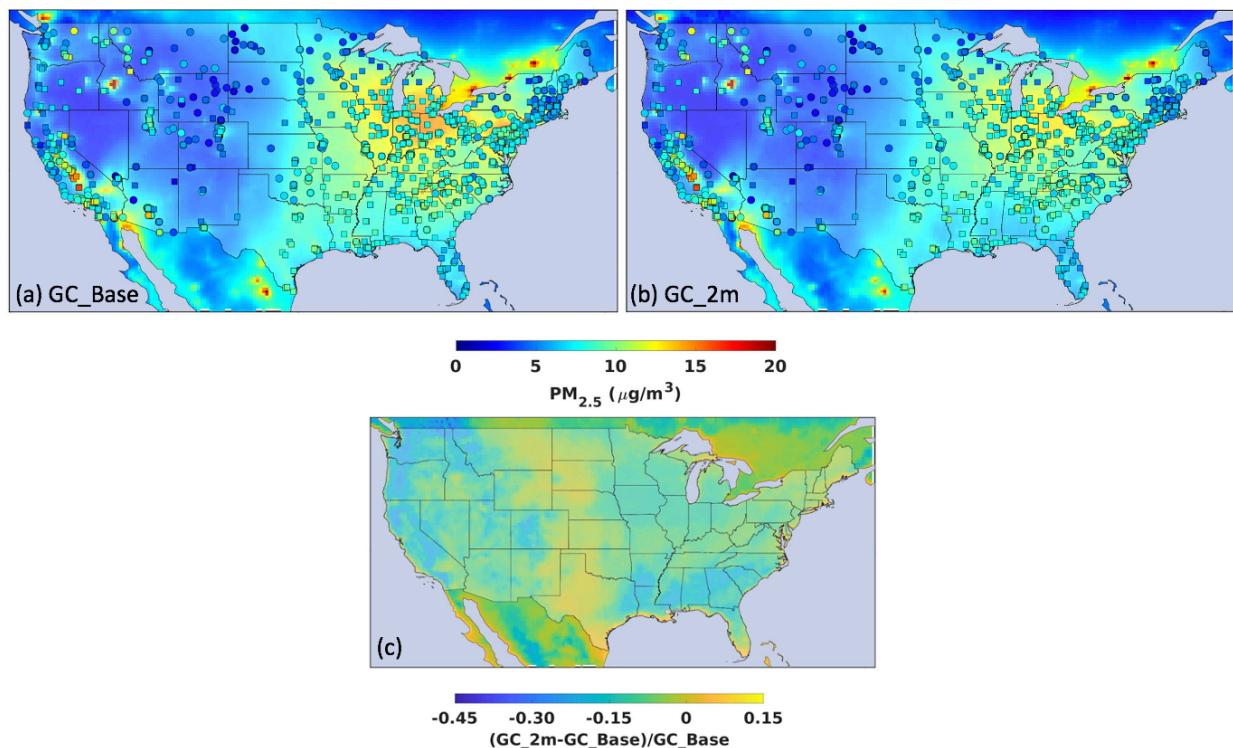


Figure S2. Annual $PM_{2.5}$ concentrations over the US in 2016. The background maps show modeled annual $PM_{2.5}$ concentrations by (a) the GC_Base simulation and (b) the GC_2m simulation. (c) The difference between GC_Base and GC_2m, calculated as $(GC_2m - GC_Base) / GC_Base$. Overlaid filled circles represent in-situ FEM measurements. Filled squares represent in-situ FRM measurements.

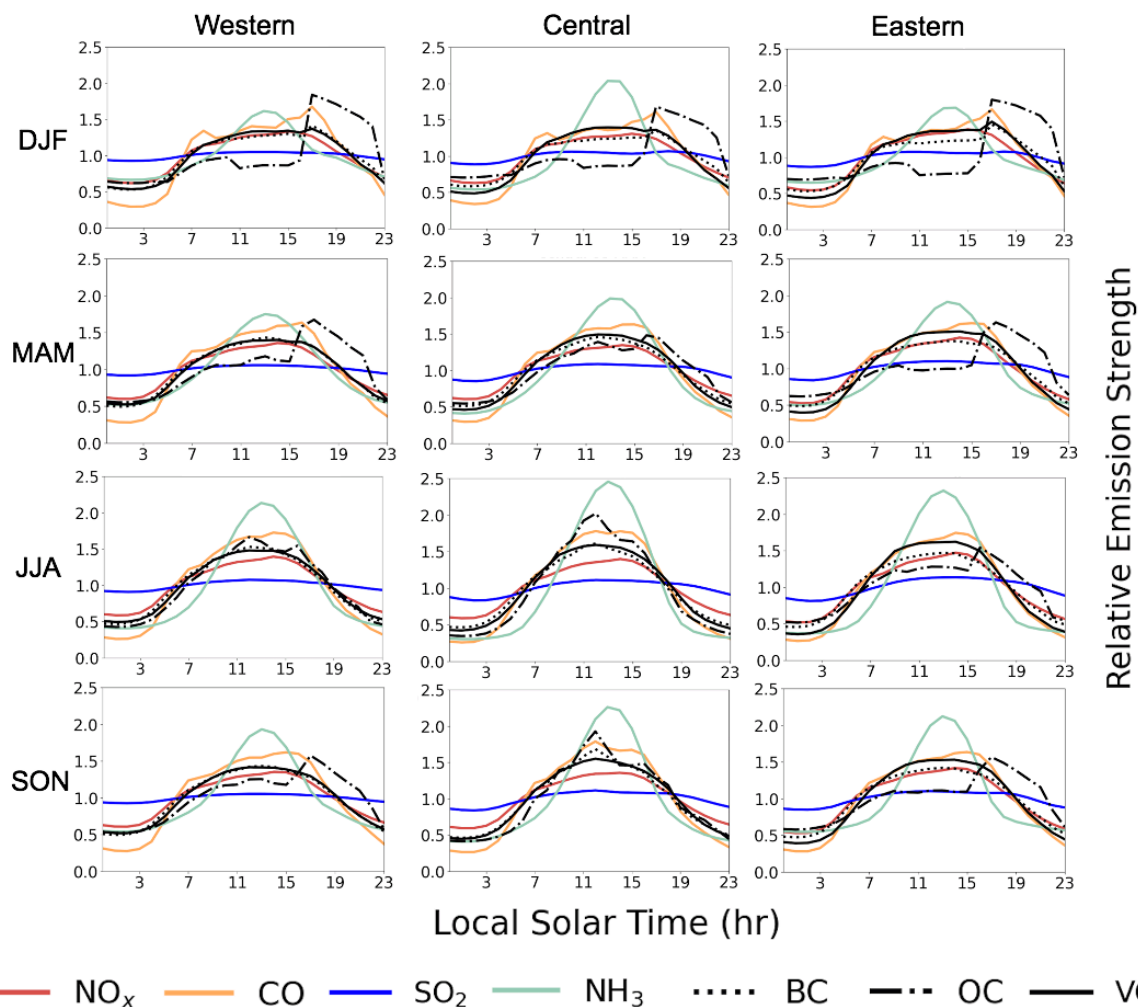


Figure S3. Normalized mean seasonal and regional diel profiles of speciated emissions from the EPA National Emission Inventory (NEI).

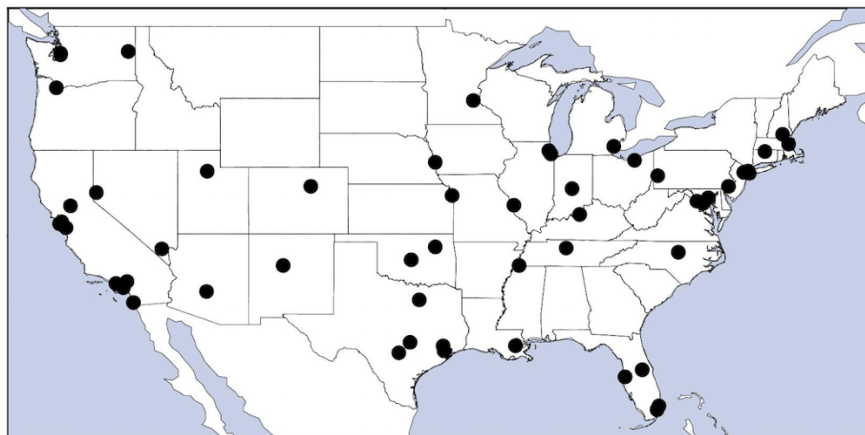


Figure S4. The Aircraft Meteorological Data Reports (AMDAR) sites.

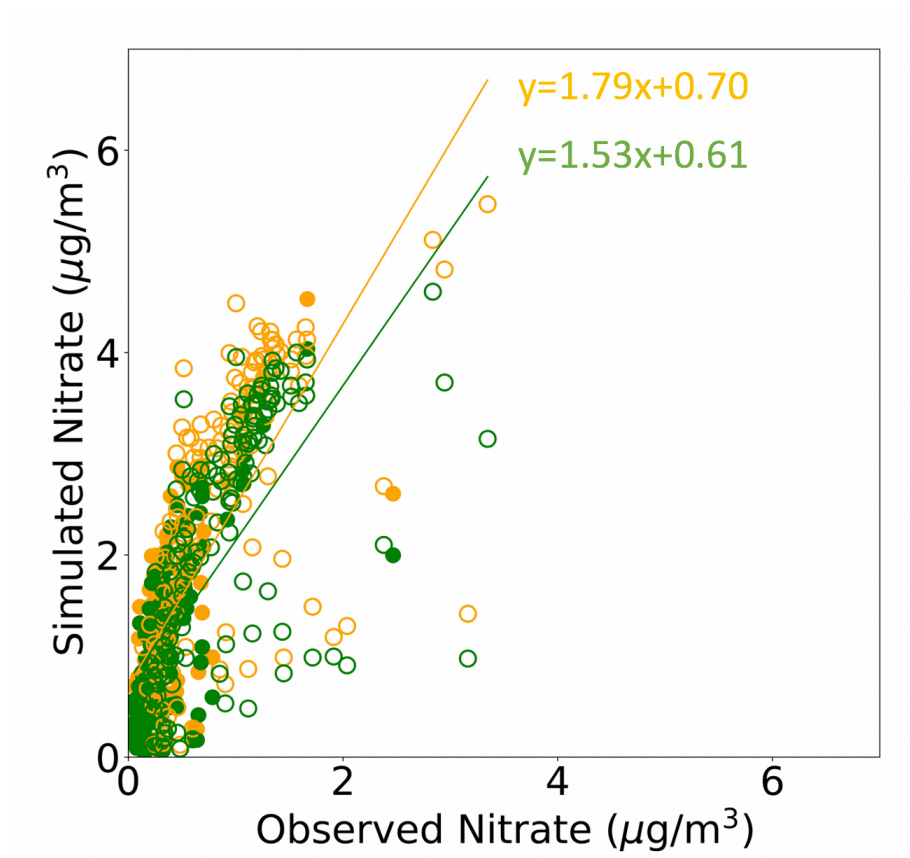


Figure S5. Mass concentrations of nitrate $\text{PM}_{2.5}$ in the GC_Base (orange) and GC_2m (green) simulations (Table 1) in 2016. The filled/hollow circles represent in situ observations from the IMPROVE/CSN network respectively.

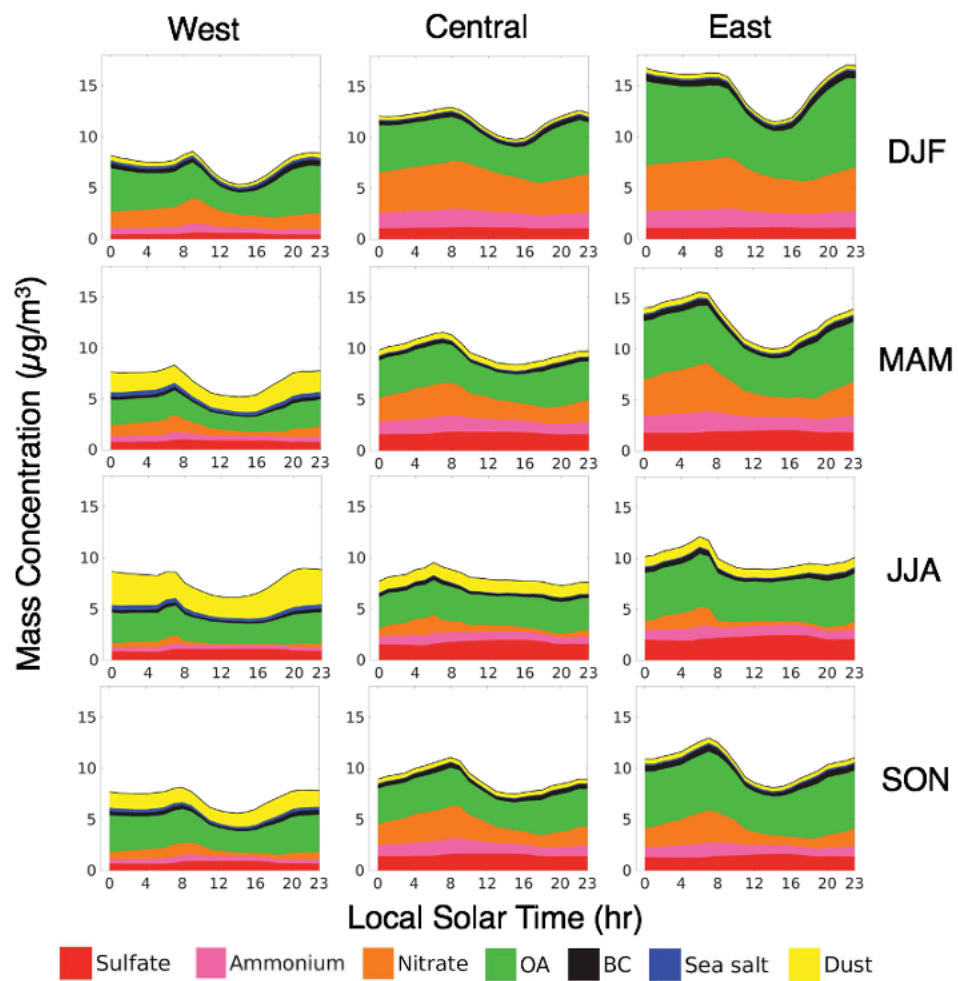


Figure S6. Seasonal and regional diel profiles of PM_{2.5} composition in the GC_2m (Table 1) simulation.

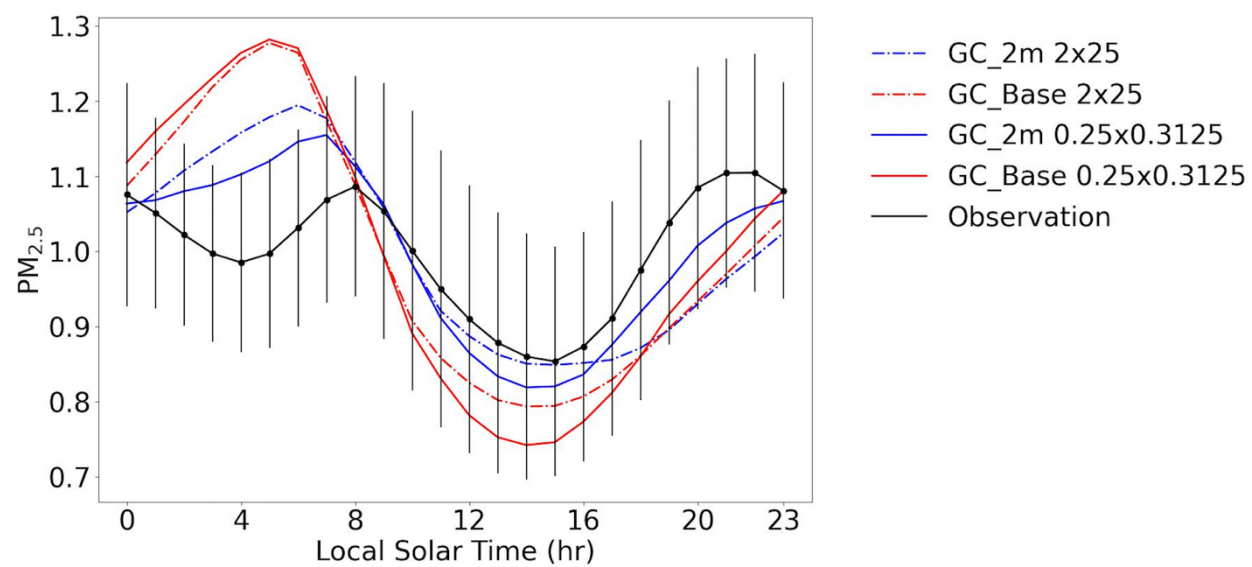


Figure S7. Diel $PM_{2.5}$ of the GC_Base and GC_2m simulations at different spatial resolution.

Table S1. RMSD of GEOS-Chem PM_{2.5} against the FEM measurements. (Unit: $\mu\text{g}/\text{m}^3$)

Region	Season	GC Base	GC Emis	GC Drydep	GC 2m
Western	DJF	1.79	1.38	1.36	2.37
	MAM	2.40	1.94	1.84	0.99
	JJA	2.08	1.63	1.50	0.98
	SON	1.82	1.32	1.26	0.50
Central	DJF	4.93	4.81	4.77	4.12
	MAM	4.10	3.77	3.71	3.18
	JJA	2.74	2.08	1.94	1.50
	SON	3.47	2.86	2.76	2.23
Eastern	DJF	6.55	6.47	6.83	6.08
	MAM	6.29	5.59	5.93	5.11
	JJA	3.86	2.81	2.98	2.35
	SON	4.33	3.58	3.78	2.95